Structural Eng./Earthquake Eng. Vol. 10, No. 2, 59s—69s, July 1993
Japan Society of Civil Engineers (J. Struct. Mech. Earthquake Eng. No. 471/I—24)

A GENERALIZED TWO-SURFACE MODEL FOR STRUCTURAL STEELS UNDER CYCLIC LOADING

Chi SHEN*, Eiji MIZUNO**
and Tsutomu USAMI***

A generalized two-surface model is proposed which can be used in multi-dimensional stress state even within the yield plateau. The description of the cyclic behavior observed in the uniaxial cyclic experiments is also included in the present model. Moreover, the proposed model has been implemented by the finite element method numerically. A good agreement between the experimental results and prediction by the proposed model has been obtained.

Key Words : *two-surface model, plasticity, cyclic behavior, hardening rule, constitutive equation.*

1. INTRODUCTION

The advanced life prediction needs nonlinear analysis of structures, especially under cyclic loading. Accordingly, with the increase of accuracy in computation methods, better constitutive equations have to be used to describe the inelastic behavior of material in the case of cyclic loading. For the ductile material, such as steel, it is favorite to adopt plasticity theory and the cyclic behavior may be evaluated to a certain extent by the classical kinematic hardening rule or mixed kinematic hardening rule. However, there are many cases in which the kinematic or mixed kinematic hardening rule in conventional plasticity theory may not give the satisfactory prediction for the cyclic behavior because some parameters related to the cyclic behavior are not properly included.

The multi-surface model is a typical example of the plasticity models for steels under cyclic loading[1),2),3),4)]. An alternative model is a two-surface model originally proposed by Dafalias·Popov[5)] and Kreig[6)] independently. One of the two surfaces is the yield surface as in conventional plasticity theory. Another is called the bounding surface which encompasses the yield surface during the plastic deformation. Recently, various modified versions of the two-surface model have been proposed by some authors[7),8),9),10)] and were successful in predicting the cyclic plasticity behavior of some materials under uniaxial or biaxial cyclic loadings. However, the yield plateau, that is one of the important characteristics of structural steel, was rarely mentioned in those two-surface models. This problem was discussed in detail and the satisfactory prediction has been obtained for the steels SS400, SM490 and SM570 under uniaxial cyclic loading in Refs. 4), 11), and 12).

In the present paper, a generalized two-surface model is proposed as an extension of the authors' previous model with the consideration of the yield plateau. Also a comparison between the experiment and prediction by the proposed model is given. The developed model could be applied to analyse the elasto-plastic cyclic behavior of locally buckled steel plate elements and thin-walled steel structures under cyclic loading.

2. REVIEW OF THE UNIAXIAL TWO-SURFACE MODEL PROPOSED BY AUTHORS

In order to obtain an accurate prediction for the cyclic behavior of structural steel even within the yield plateau(for example, path OABCDE in **Fig.1**), the authors proposed a uniaxial two-surface model in Refs. 11), 12) and 13), which included the following features:

1) In the calculation of the plastic modulus E^P, the same equation as in the Dafalias·Popov[5)] model was used.

$$E^P = E^P_{0i} + h\frac{\delta}{\delta_{in} - \delta} \quad \cdots\cdots\cdots\cdots\cdots\cdots (1)$$

where E^P_{0i} = the slope of the bounding line(say, $X - X'$, $Y - Y'$ and $Z - Z'$ in **Fig.1**) for the

* Member of JSCE, Dr. Eng., Research Associate, Dept. of Civil and Environmental Engineering, Saitama University, Urawa, 255, JAPAN
** Member of JSCE, Ph.D., Associate Professor, Dept. of Civil Engineering, Nagoya University, Nagoya, 464, JAPAN
*** Member of JSCE, Dr. Eng., D.Sc., Professor, Dept. of Civil Engineering, Nagoya University, Nagoya, 464, JAPAN

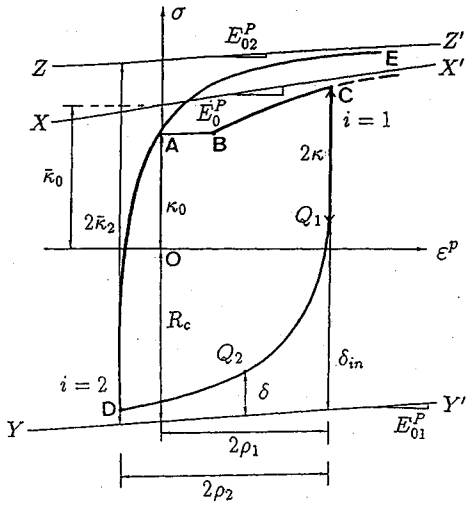

Fig. 1 Uniaxial cyclic stress σ versus plastic strain ε^p curve

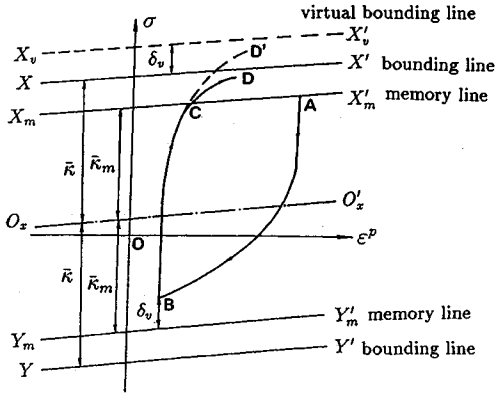

Fig. 2 Virtual bounding line and memory line

ith loading path which will be given later; h = the shape parameter; δ = the distance between the bounding line and loading point(point Q_2 in **Fig.1**) and δ_{in} = the value of δ at the initiation of a yielding process(point Q_1 in **Fig.1**).

2) The shape parameter h is assumed to be a linear function of δ, i.e.,

$$h = e \cdot \delta + f \quad \cdots\cdots\cdots\cdots\cdots\cdots\cdots\cdots (2)$$

where e and f are constants.

3) The following expression of the elastic range, 2κ, is obtained from the experimental data.

$$\kappa/\kappa_0 = \alpha - a \cdot \exp(-b\bar{\varepsilon}^p \times 100) - (\alpha - a - 1) \cdot \exp(-c\bar{\varepsilon}^p \times 100) \quad \cdots\cdots\cdots\cdots\cdots\cdots\cdots\cdots (3)$$

where κ_0 is equal to the yield stress σ_y; α, a, b and c are constants; $\bar{\varepsilon}^p$ is called accumulated effective plastic strain(A.E.P.S.), which is defined as the amplitude of the plastic strain that the material has ever experienced before and can be expressed as follows:

$$\bar{\varepsilon}^p = \varepsilon_{max}^p - \varepsilon_{min}^p \quad \cdots\cdots\cdots\cdots\cdots\cdots\cdots\cdots (4)$$

4) When the absolute value of stress reaches the initial yield stress σ_y, it is judged whether the loading point moves on the yield plateau or enters the hardening range with E^P by the following rule; If:

$$(\frac{\bar{\varepsilon}^p}{\varepsilon_{st}^p} - 1) < M \cdot (\frac{W^P}{W_{st}^P} - 1) \quad \cdots\cdots\cdots\cdots\cdots\cdots (5)$$

then yield plateau still continues, otherwise, yield plateau disappears, where W_{st}^P and ε_{st}^p represent the plastic work and plastic strain at the end of the yield plateau under monotonic loading respectively; M is a constant.

5) The size of the bounding surface, $\bar{\kappa}$ is a function of A.E.P.S.

$$\bar{\kappa} = \bar{\kappa}_\infty + (\bar{\kappa}_0 - \bar{\kappa}_\infty) \cdot \exp(-\zeta \cdot \rho^2) \quad \cdots\cdots\cdots\cdots (6)$$

where $\bar{\kappa}_\infty$ is the limit size of the bounding surface and assumed to be the ultimate tensile stress σ_u; $\rho = \frac{1}{2}\bar{\varepsilon}^p$; $\bar{\kappa}_0$ indicates the height of the initial bounding line and ζ is a constant.

6) The virtual bounding line and memory line are used to predict the stress-strain curve BCD from point B, where the reversed loading occurs before the unloading path AB reaches the memory line $Y_mY'_m$, as shown in **Fig.2**.

The initial memory line is set to pass the initial yield stress σ_y and have the smae slope as that of the bounding line. As the stress increases up to point A(as shown in **Fig.2**), the memory line also moves together with the loading point. Supposing that line $O_xO'_x$ is the center line of the bounding lines XX' and YY', the memory lines $X_mX'_m$ and $Y_mY'_m$ in tension and compression sides are assumed to be parallel to the real bounding line and be symmetry with respect to the center line $O_xO'_x$. The loading point A on the memory line $X_mX'_m$ represents the point of

the maximum stress that the material has ever experienced before.

When the reversed loading point, such as point B in **Fig.2**, does not reach the memory line, the virtual bounding line $X_vX'_v$ will be used in the prediction of path BC. The virtual bounding line $X_vX'_v$ is assumed to shift from the bounding line XX' by a distance δ_v which is measured from the reversed loading point B to the memory line $Y_mY'_m$. The radius of the virtual bounding lines is assumed to be:

$$\bar{\kappa}_v = \bar{\kappa} + \delta_v \quad \cdots\cdots (7)$$

In the prediction of path BC, the plastic modulus E^P is calculated as follows:

$$E^P = E^P_{0i} + h\frac{\delta + \delta_v}{(\delta_{in} + \delta_v) - (\delta + \delta_v)} \quad \cdots\cdots (8)$$

However, once the loading point reaches the memory line, such as point C in **Fig.2**, the plastic modulus in the continuous path CD instead of CD' is calculated by Eq.(1).

7) The slope of the bounding line is found to decrease with the plastic work in the cyclic experiments. In this model, the bounding line slope of the ith loading path has the following expression.

$$E^P_{0i}(W^P_i) = \frac{E^P_0}{1 + \omega W^P_i} \quad \cdots\cdots (9)$$

where ω is a constant; E^P_0 is the slope of the initial bounding line and determined from the monotonic loading experiment; W^P_i is the plastic work accumulated from the origin point O to the ith reversed loading point(as shown in **Fig.1**, i=1 for point C and i=2 for point D).

3. PROPOSAL OF THE TWO-SURFACE MODEL FOR MULTIAXIAL STRESS STATE

In the present paper, the uniaxial two-surface model proposed by the authors is extended to the multi-dimensional stress state. All the parameters mentioned in section 2 are introduced by giving a proper generalized definition. Moreover, to describe the stress state in the multiaxial case, the yield surface, bounding surface and the corresponding hardening rule have to be considered.

(1) Extension of A.E.P.S. to Multiaxial Stress State

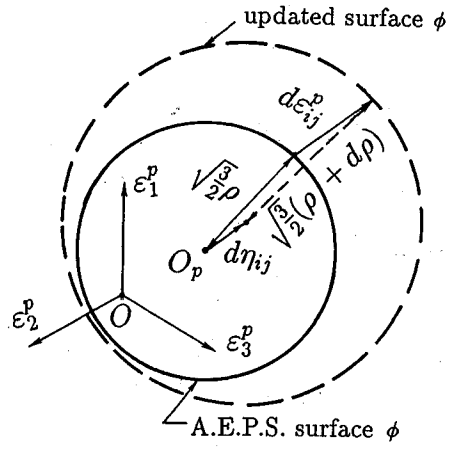

Fig. 3 Definition of A.E.P.S. surface

As explained in section 2, the calculations of the parameters κ, $\bar{\kappa}$ and the yield plateau are all related to A.E.P.S. concept. To extend this concept to the multiaxial stress state, a surface defined in the plastic strain space[14),15)] is introduced and expressed as follows:

$$\phi(\varepsilon^p_{ij}) = \frac{2}{3}(\varepsilon^p_{ij} - \eta_{ij})(\varepsilon^p_{ij} - \eta_{ij}) - \rho^2 = 0 \quad \cdots\cdots (10)$$

where ε^p_{ij} is the component of plastic strain; η_{ij} and ρ represent the center and radius of the surface respectively. Here the surface ϕ is called the *A.E.P.S.* surface for convenient. During the plastic deformation, A.E.P.S. surface moves and changes in size conditionally, as shown in **Fig.3**.

According to the definition of A.E.P.S. in the uniaxial case, the multi-dimensional motion of A.E.P.S. surface may be defined as follows:

$$d\eta_{ij} = \begin{cases} \frac{1}{2}d\varepsilon^p_{ij} & \text{if } \phi(\varepsilon^p_{ij} + d\varepsilon^p_{ij}) > 0 \\ 0 & \text{otherwise} \end{cases} \quad \cdots\cdots (11)$$

From the condition $d\phi = 0$, there exists:

$$\frac{2}{3}(\varepsilon^p_{ij} - \eta_{ij})(d\varepsilon^p_{ij} - d\eta_{ij}) - \rho d\rho = 0 \quad \cdots\cdots (12)$$

Then substituting Eq.(11) into Eq.(12) yields:

$$d\rho = \begin{cases} \frac{1}{3}(\varepsilon^p_{ij} - \eta_{ij})d\varepsilon^p_{ij}/\rho & \text{if } \phi(\varepsilon^p_{ij} + d\varepsilon^p_{ij}) > 0 \\ 0 & \text{otherwise} \end{cases} \quad \cdots\cdots (13)$$

It should be noted that the initial increment of ρ, $d\rho$, is calculated as follows after the material is initially yielded.

$$d\rho = \frac{1}{2}d\varepsilon^p = \frac{1}{2}\sqrt{\frac{2}{3}d\varepsilon^p_{ij}d\varepsilon^p_{ij}} \quad \cdots\cdots (14)$$

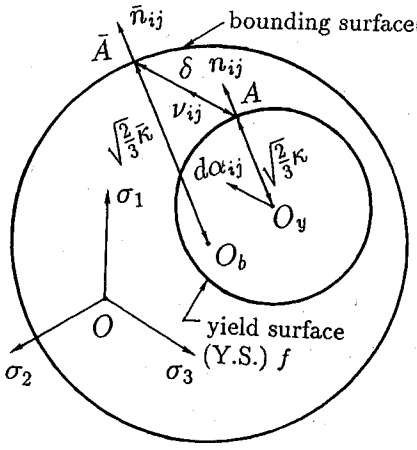

$O_b(\beta_{ij})$: center of B.S.; $O_y(\alpha_{ij})$: center of Y.S.

$\bar{A}(\bar{S}_{ij})$: conjugate point on B.S.

$A(S_{ij})$: loading point on Y.S.

$\|A\bar{A}\| = \delta$

$O_b\bar{A}$ is parallel to O_yA; $d\alpha_{ij}$ is parallel to $A\bar{A}$

Fig. 4 Yield and bounding surfaces

In the uniaxial case, it can be seen that ρ is one half of A.E.P.S., i.e., $\rho = \frac{1}{2}\bar{\varepsilon}^p$. Therefore, all the equations mentioned in the Section 2 related to A.E.P.S. can also be used in the multiaxial stress state by substituting 2ρ for $\bar{\varepsilon}^p$.

(2) Definition of Yield and Bounding Surfaces

For steel, the von Mises yield criterion is usually used in the plasticity analysis. Here the Mises yield function is adopted to describe the yield and bounding surfaces(see **Fig.4**).

Yield surface:

$$f(\sigma_{ij}, \alpha_{ij}, \kappa) = \frac{3}{2}(S_{ij} - \alpha_{ij})(S_{ij} - \alpha_{ij}) - \kappa^2 = 0 \quad \cdots\cdots (15)$$

Bounding surface:

$$F(\sigma_{ij}, \beta_{ij}, \bar{\kappa}) = \frac{3}{2}(S_{ij} - \beta_{ij})(S_{ij} - \beta_{ij}) - \bar{\kappa}^2 = 0 \quad \cdots\cdots (16)$$

where σ_{ij} and S_{ij} are the stress and deviatoric stress components; κ and $\bar{\kappa}$ represent the radii of the loading and bounding surfaces which are calculated by Eqs.(3) and (6) respectively by substituting 2ρ for $\bar{\varepsilon}^p$; α_{ij} and β_{ij} indicate the centers of the two surfaces. These two surfaces move and change in size with the plastic deformation.

(3) Definition of δ

The definition of δ is one of the most important problems in the two-surface model since it is related to the calculation of plastic modulus, as in Eq.(1). In fact, the definition of δ in the multi-dimensional stress state corresponds to a proper mapping rule between the two surfaces. In the Dafalias· Popov[5] model, the mapping rule associates σ_{ij} and $\bar{\sigma}_{ij}$ with the same normal on the two surfaces and δ is measured by the Euclidean norm. On the other hand, Tseng·Lee[7] assumed that the center of bounding surface does not move and only expands isotropically. Moreover, δ is measured by the Euclidean norm in the deviatoric stress space from the loading point to the bounding surface along the direction of the stress increment. In the present paper, the Dafalias·Popov mapping rule is adopted(see **Fig.4**), i.e.,

$$\frac{\bar{S}_{ij} - \beta_{ij}}{\sqrt{\frac{2}{3}}\bar{\kappa}} = \frac{S_{ij} - \alpha_{ij}}{\sqrt{\frac{2}{3}}\kappa} \quad \cdots\cdots (17)$$

and

$$\delta = \sqrt{\frac{3}{2}}\|\bar{S}_{ij} - S_{ij}\| \quad \cdots\cdots (18)$$

where $\bar{S}_{ij}$ represents the deviatoric stress components of point $\bar{A}$ on the bounding surface.

(4) Hardening Rule of the Yield Surface

In the two-surface model, the hardening rule usually depends on the definition of δ to ensure that they will be tangential to each other when the two surfaces contact. In the Dafalias· Popov model, it was assumed that the center of the loading surface moves along the direction connecting the two conjugate points $A\bar{A}$ in **Fig.4**. The hardening rule in the Dafalias·Popov model is adopted in the present paper:

$$d\alpha_{ij} = C_\alpha \cdot \nu_{ij} \quad \cdots\cdots (19)$$

where C_α is a scalar; ν_{ij} is a unit vector along $A\bar{A}$ and can be expressed as follows:

$$\nu_{ij} = \sqrt{\frac{3}{2}}\frac{\bar{S}_{ij} - S_{ij}}{\delta} \quad \cdots\cdots (20)$$

Then substituting Eq.(19) into the following consistency equation, $df = 0$,

$$df = 3(S_{ij} - \alpha_{ij})dS_{ij} - 3(S_{ij} - \alpha_{ij})d\alpha_{ij} - 2\kappa \cdot d\kappa = 0 \quad \cdots\cdots (21)$$

C_α is obtained as follows:

$$C_\alpha = \frac{(S_{ij} - \alpha_{ij})dS_{ij} - \frac{2}{3}\kappa \cdot d\kappa}{(S_{ij} - \alpha_{ij})\nu_{ij}} \quad \cdots\cdots (22)$$

It should be noted that when the two surfaces contact, i.e., $\delta = 0$, Eq.(20) can not be used. Therefore, we determine α_{ij} from the condition that the two surfaces are tangential to each other:

$$\frac{S_{ij} - \alpha_{ij}}{\kappa} = \frac{S_{ij} - \beta_{ij}}{\bar{\kappa}} \quad \cdots\cdots (23)$$

Then

$$\alpha_{ij} = S_{ij} - \frac{\kappa}{\bar{\kappa}}(S_{ij} - \beta_{ij}) \quad \cdots\cdots (24)$$

(5) Motion of the Bounding Surface

In the uniaxial case, the center of the two bounding lines, β, can be calculated as follows:

$$d\beta = E_0^P \cdot d\varepsilon^p - d\bar{\kappa} \cdot \frac{\bar{\sigma} - \beta}{\bar{\kappa}} \quad \cdots\cdots (25)$$

Following the definition of the effective stress, we assume the relationship between $d\beta$ and $d\beta_{ij}$ to have the similar expression:

$$d\beta = \sqrt{\frac{3}{2} d\beta_{ij} d\beta_{ij}} \quad \cdots\cdots (26)$$

As an extension of Eq.(25), the motion of the bounding surface is here assumed as:

$$d\beta_{ij} = C_1 \cdot d\varepsilon_{ij}^p + C_2 \cdot n_{ij} \quad \cdots\cdots (27)$$

where C_1 and C_2 are scalars; n_{ij} represents the unit normal of the loading surface at the current stress point; $d\varepsilon_{ij}^p$ indicates the increment of the plastic strain. According to the associated flow rule of plasticity theory, we have

$$d\varepsilon_{ij}^p = \|d\varepsilon_{ij}^p\| n_{ij} \quad \cdots\cdots (28)$$

By substituting Eq.(28) into Eq.(27) and comparing the resulting equation with Eq.(25), it can be obtained that

$$C_1 = \frac{2}{3} E_0^P \quad \text{and} \quad C_2 = -\sqrt{\frac{2}{3}} d\bar{\kappa} \quad \cdots\cdots (29)$$

where Eq.(26) and the following definition of the effective plastic strain increment have been used

$$d\varepsilon^p = \sqrt{\frac{2}{3} d\varepsilon_{ij}^p d\varepsilon_{ij}^p} \quad \cdots\cdots (30)$$

Therefore, the motion of the bounding surface can be expressed as follows:

$$d\beta_{ij} = \frac{2}{3} E_0^P \cdot d\varepsilon_{ij}^p - \sqrt{\frac{2}{3}} d\bar{\kappa} \cdot n_{ij} \quad \cdots\cdots (31)$$

It can be known that the bounding surface is also hardened in a combined form.

(6) Introduction of Virtual Bounding Surface and Memory Surface

The virtual bounding line and memory line in the uniaxial case are here extended to a virtual bounding surface and memory surface, respectively. It is assumed that the virtual bounding surface and the memory surface have the same center as the real bounding surface(see **Fig.5**). The size of the memory surface is updated with the distance between the stress point S_{ij} and the center of the bounding surface, i.e.,

$$\bar{\kappa}_m = \{\sqrt{\frac{3}{2}} \|S_{ij} - \beta_{ij}\|\}_{max} \quad \cdots\cdots (32)$$

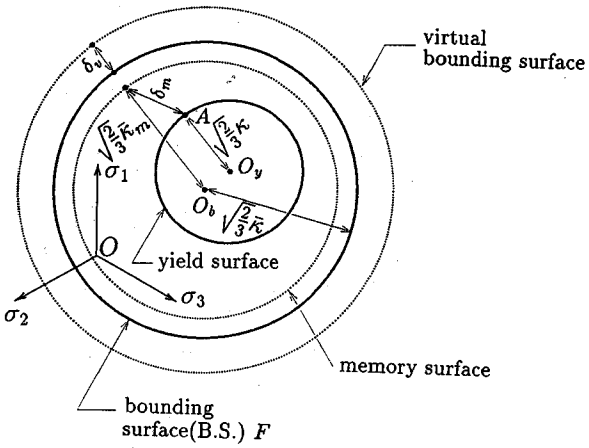

Fig. 5 Virtual bounding surface and memory surface

Supposing that the distance between the loading point A and the memory surface is denoted by δ_m as shown in **Fig.5**, δ_m is taken as δ_v when the loading is reversed.

(7) Constitutive Equation

By combining the hardening rule and the plastic modulus with the plasticity theory, the constitutive equation can be established easily. With the assumption of small deformation, the elasto-plastic stress and strain relation in an incremental form can be written as follows:

$$d\sigma_{ij} = D_{ijkl} d\varepsilon_{kl} \quad \cdots\cdots (33)$$

where

$$D_{ijkl} = \mu(\delta_{ik}\delta_{jl} + \delta_{ij}\delta_{kl}) + \lambda\delta_{ij}\delta_{kl} - \frac{1}{\kappa^2} \cdot \frac{9\mu^2}{E^P + 3\mu}(S_{ij} - \alpha_{ij})(S_{kl} - \alpha_{kl}) \quad \cdots\cdots (34)$$

in which λ and μ are the Lame's coefficients; E^P is calculated by Eq.(1) or Eq.(8). In this constitutive equation, the nonlinear hardening is included.

4. APPLICATION OF THE PRESENT MODEL

(1) Outline of the Experiment

To examine the applicability and the accuracy of the proposed model, some tests have been carried out under cyclic tension-compression loading. The cyclic experiment was done for two kinds of specimens as shown in **Fig.6**.

The sections of the specimens are in circular form, but not uniform in longitudinal direction. All the

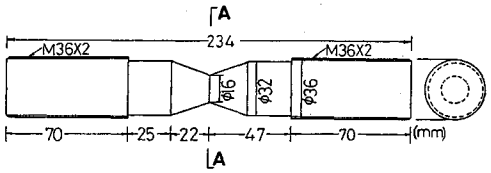

(a) specimen of type A

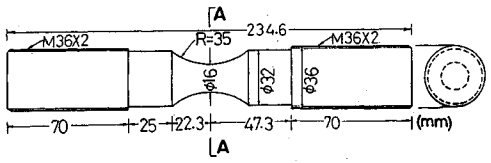

(b) specimen of type B

Fig. 6 Test specimens

Table 1 The Model Parameters of Steel SS400

Parameter	Value	Parameter	Value
E(GPa)	206.7	σ_y(MPa)	274.4
E^p_{st}/E	0.025	ε^p_{st}	0.0153
a	-0.505	b	2.17
c	14.4	α	0.191
e	500.0	f/E	0.30
E^p_0/E	8.96×10^{-3}	$\omega\cdot\sigma_y$	3.08
$\bar{\kappa}_0/\sigma_y$	1.15	σ_u/σ_y	1.81
$\zeta\cdot\varepsilon^2_y$	9.89×10^{-4}	M	-0.37

Note:
E: Young's Modulus; σ_y: initial yield stress;
E^P_{st}: plastic modulus of the initial hardening at point B in **Fig.1**; $\varepsilon_y = E/\sigma_y$

specimens are made of the same steel SS400. Numbers of specimens are 7 for each type. A cyclic tension and compression loads act on the specimens in the longitudinal direction uniaxially.

The testing machine used in the experiments is the MTS810 with 25tonf loading capacity, where the stretch of specimen in longitudinal direction was measured with an extensometer in 50mm length and the experimental data were recorded by a computer simultaneously. In addition, the load-displacement curve was drawn in X-Y plotter. During the experiment, the loading process was controlled by displacement with a very lower speed of $10^{-4}(mm/mm)/min$. Based on the uniaxial cyclic experimental results[11),12)], the parameters of the proposed model for steel SS400 have been obtained as shown in **Table 1**.

(2) Experimental Results and Predictions with the Proposed Model

In order to predict the experimental results, the proposed model has been numerically implemented by finite element method. The computer program was completed based on FEAP81[16)], in which only the element stiffness matrix and the constitutive relation are required to be written by the users. In the computation, the Newton-Raphson method is adopted to solve the nonlinear stiffness equations and 2×2 Gauss points are used in the numerical integral.

Since the sections of all the specimens are in the circular form and the specimens are subjected to the uniaxial cyclic loading, they can be treated as an axisymmetrical problem. The stress components in the specimens are σ_z (axial stress), σ_r(radial stress), τ_{rz}(shear stress acting in r-z plane, see **Fig.7**) and σ_θ(circumferential stress).

The meshes of 4-node isoparametric element[16)], as shown in **Fig.7** are employed in the numerical analysis, where only the half of the specimen is considered with respect to section A-A.

The distribution of the stress components such as σ_z, σ_r and σ_θ on the section A-A of the specimen type B is shown in **Fig.8**. It can be found that the stress distribution changes with the increase in load P. However, the stress σ_r near the outside on section A-A almost remais zero.

The loads at the initial yielding point are 45.08KN and 52.9KN in the specimens of type A and B, respectively. Apparently, the initial yielding load in the specimen of type A is smaller than that of type B because of the stress concentration. However, with the plastic deformation and strain hardening, the loading capacity of specimen of the type A is higher than that of specimen of type B. When the all of the Gaussian points near section A-A are yielded, the plastic flow, i.e., the yield plateau can be observed from the load-displacement curve(as shown in **Fig.11**). In this case, the loads of the two types specimens are P=77.4KN in type A and P=60.7KN in type B, respectively.

The propagation of the yield zone with the increase in loading are shown in **Figs.9** and **10** for each type of the specimens.

In **Figs.11** and **12**, the load-displacement curves predicted by the present model are compared with the experimental results for the different loading histories. The effect of the yield plateau and the expansion of the bounding surface can be found in the examples.

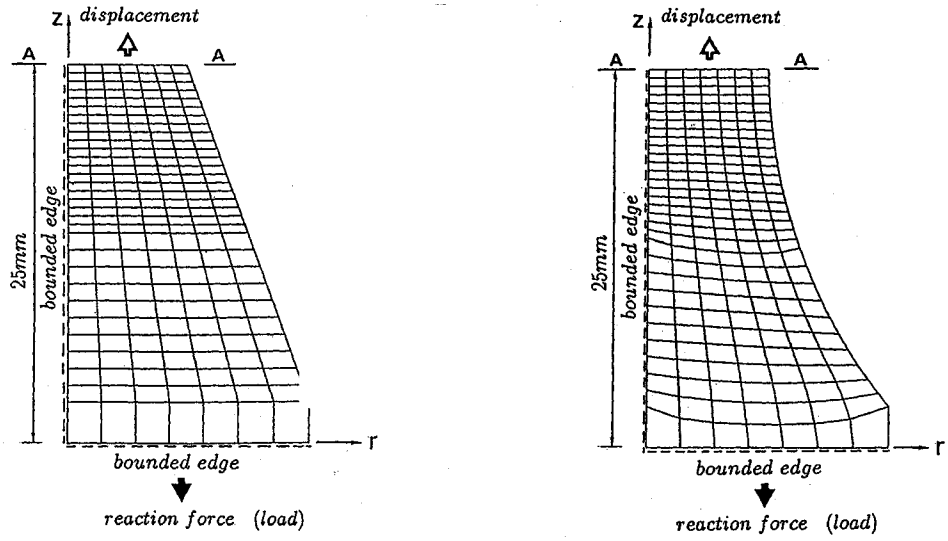

(a) mesh of type B (b) mesh of type C

Fig. 7 FEM meshes of specimens

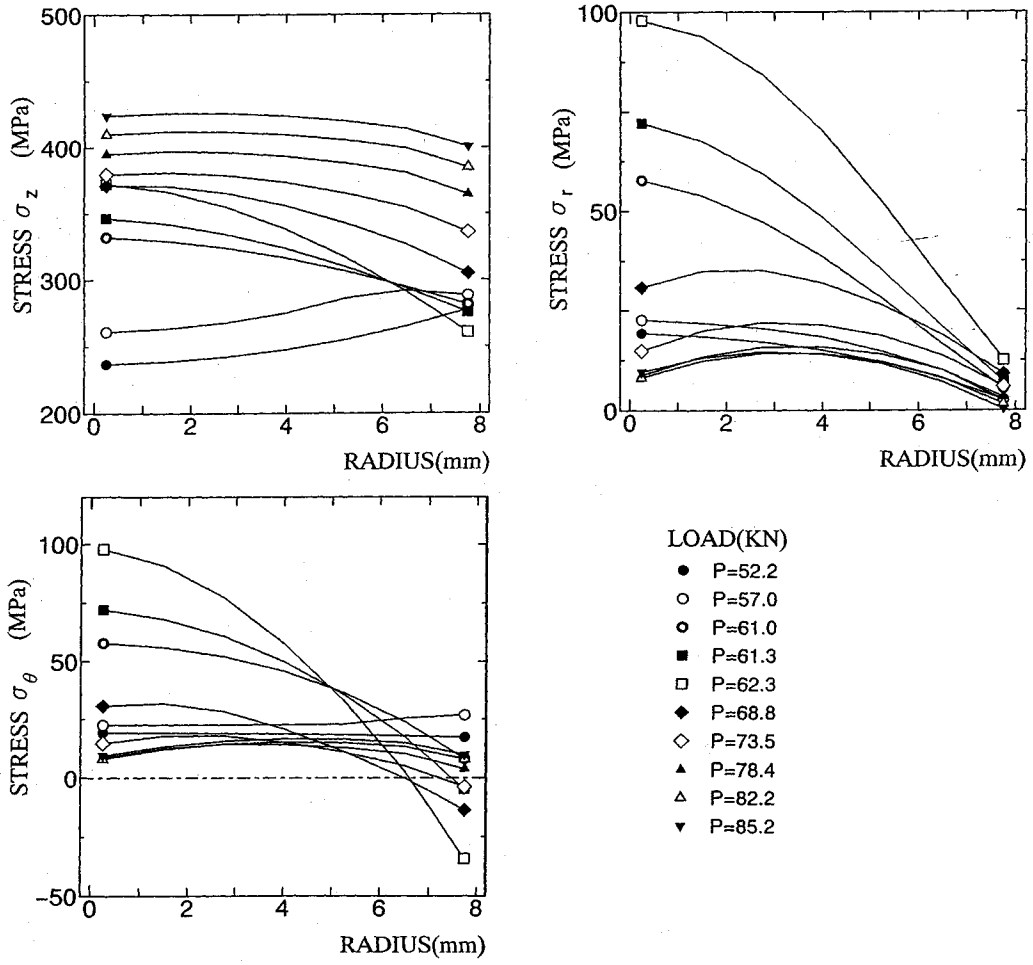

Fig. 8 Stress distribution on section A-A of specimen B-1

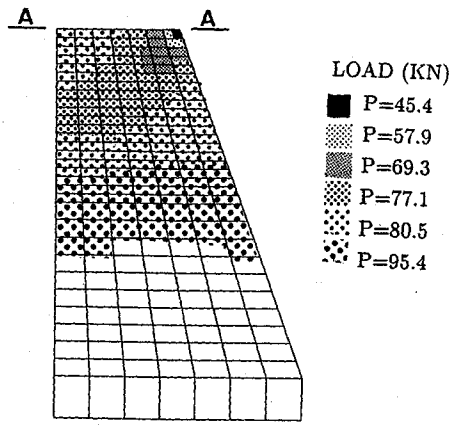

Fig. 9 Propagation of yield zone in specimen A-1

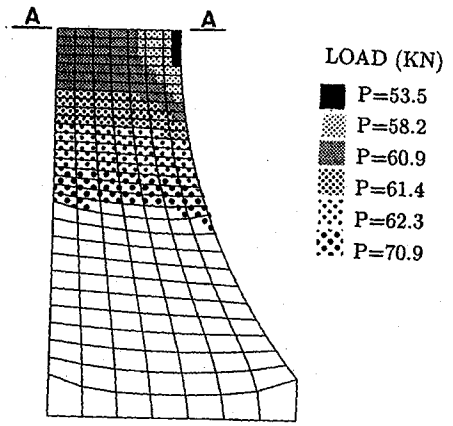

Fig. 10 Propagation of yield zone in specimen B-1

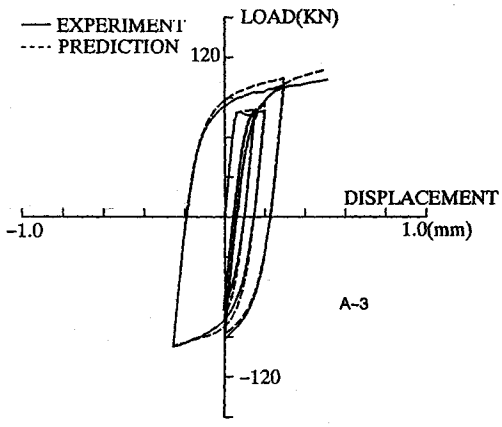

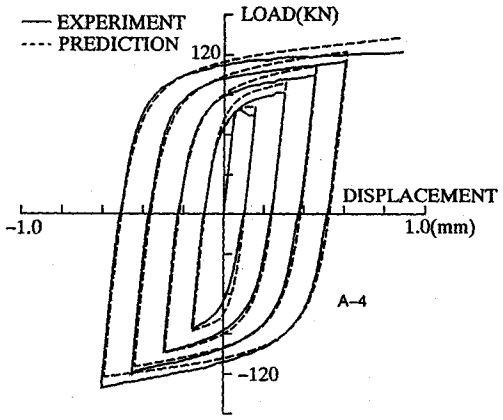

Fig. 11 Comparison between experiment and prediction of type A specimens

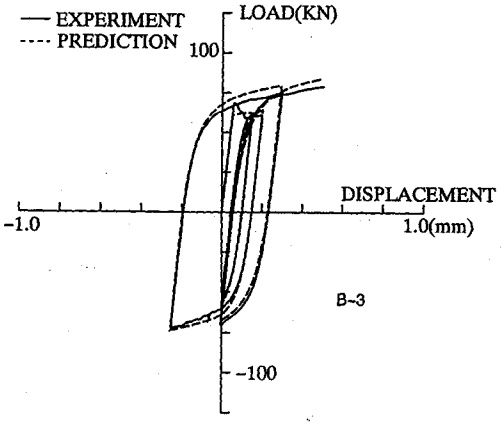

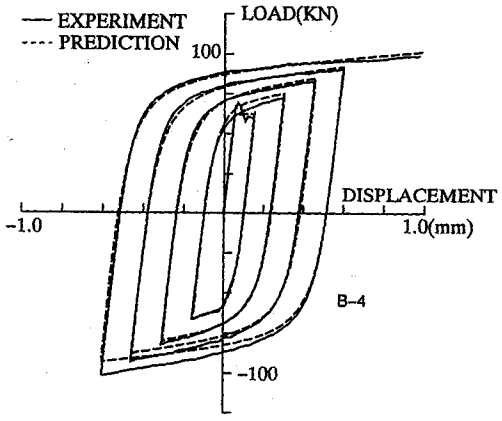

Fig. 12 Comparison between experiment and prediction of type B specimens

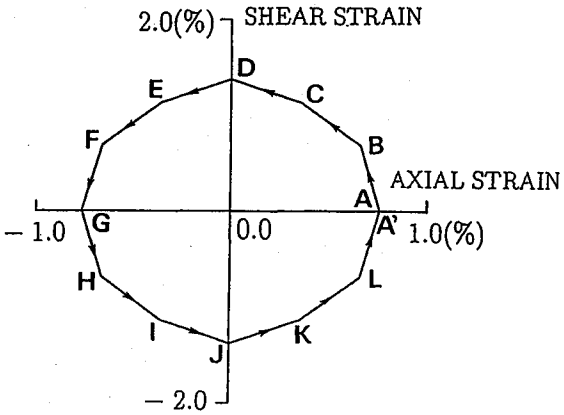

Fig. 13 Strain history in experiment (loading type II)[17]

(3) Prediction of Nonproportional Loading Case

For the wide use of the present model, the prediction of the nonproportional loading case is also done and compared with the experimental results obtained by Chang[17),18)]. The test specimens were thin-walled circular tubes and made of annealed steel ASTM A-36.

The experiment started first with the uniaxial cyclic loading under a constant amplitude of 0.8% axial strain in tension and compression sides until the material reached a stabilized state (loading type I). Then, the axial strain-shear strain path in 90°-out-of-phase were adopted in the experiment(loading type II), as shown in **Fig.13**. Although the strains changed cyclically during loading type II, the material was always in loading state. The comparisons between the experimental data(dots) and predictions(solid lines) of loading type I and II by Chang are shown in **Figs.14**(a) through **16**(a). Besides, the predictions by the present model are shown in **Figs.14**(b) through **16**(b).

The material parameters shown in Refs. 17) and 18) are Young's modulus $E = 28,500$ksi(196.5GPa), initial yield stress $\kappa_0 = \sigma_y = 30$ksi(206.9MPa), length of yield plateau(plastic strain) $\varepsilon^p_{st} = 1.6\%$, yield stress in the cyclic loading $= \alpha \times \kappa_0 = 20$ksi(137.9MPa) and $E^P_0 = 500$ksi(3.45GPa). The other model parameters needed in the prediction by the present model can be obtained from **Table 1** using E and σ_y given above. The present model is accurate enough to predict the axial stress-axial strain relation(**Fig. 14**(b)) and shear stress-shear strain relation(**Fig.16** (b)). However, the axial stress predicted during loading type II, as shown in **Fig.15**(b), is lower than that of experiment. Considering the fact that the material used in the experiment is an annealed steel, the present model seems to predict well the experimental results.

In the present model, the effect of the additional hardening[19)] under onoproportional cyclic loading is not considered. However, the additional hardening in the above nonproportional experiment is not so serious and can be neglected.

5. SUMMARY AND CONCLUSIONS

From the comparison between the prediction and the experimental data, it can be concluded that the proposed model can be used to predict the cyclic behavior of structural steels in multi-dimensional stress state, even for cyclic behavior within yield plateau. Moreover, the present model can also be used in the case of nonproportional loading under biaxial stress state. With the extension of the A.E.P.S. concept into the multi-dimensional state, the calculation of the parameters in the uniaxial case can be introduced in the present model easily, such as the the yield plateau, the elastic range and the size of the bounding surface. All the parameters used in the present model are obtained from the uniaxial cyclic loading experiments. By combining the present model with the plasticity theory, the incremental constitutive relationship is obtained. In addition, the equations in this model are consistent with those in uniaxial two-surface model. With the help of program FEAP81[16)], the prediction of the steel structures under cyclic loading can be done by introducing the proper element in this model.

In summary, the applicability and accuracy of the proposed model can be demonstrated by the above numerical examples. Moreover, it is expected that

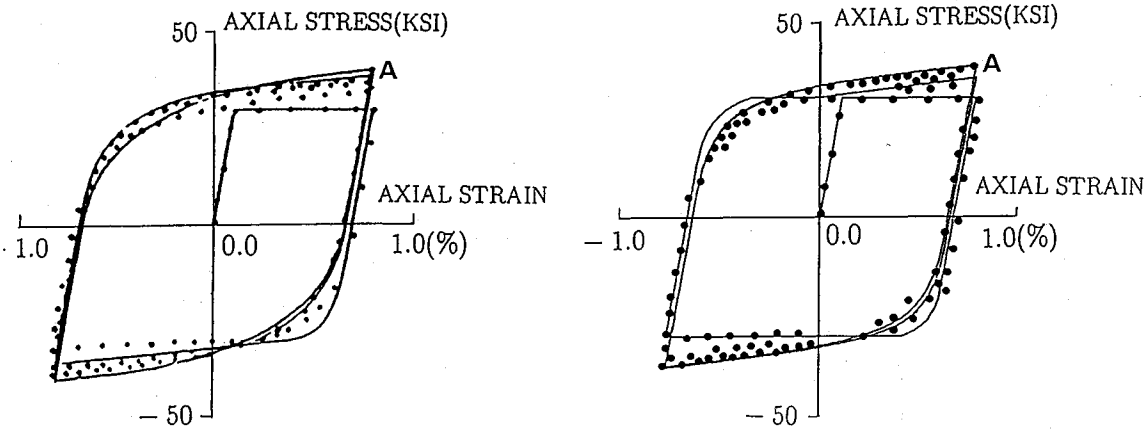

(a) (•) experiment; (–) prediction by Chang[17] (b) (•) experiment; (–) prediction by present model

Fig. 14 Axial stress σ-axial strain ε curves(loading type I)

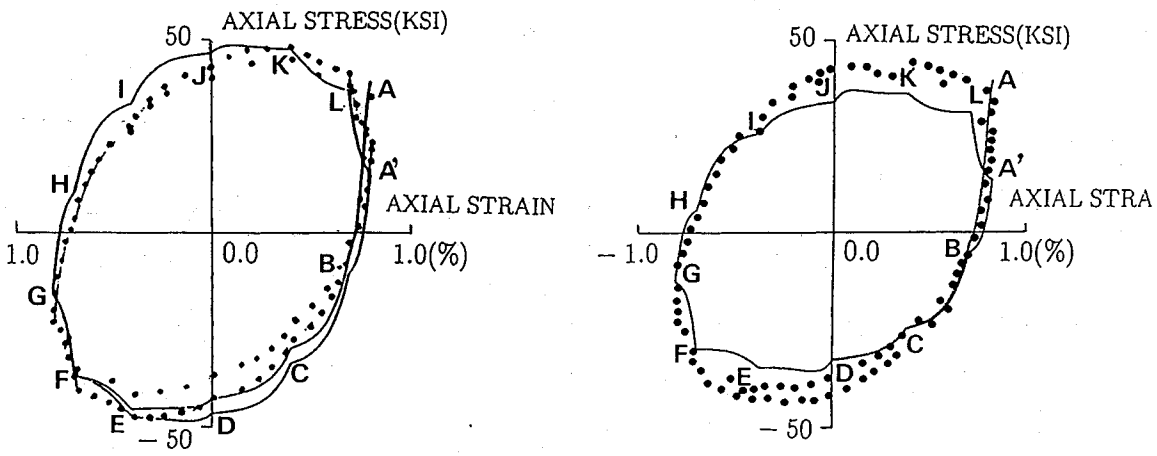

(a) (•) experiment; (–) prediction by Chang[17] (b) (•) experiment; (–) prediction by present model

Fig. 15 Axial stress σ-axial strain ε curves(loading type II)

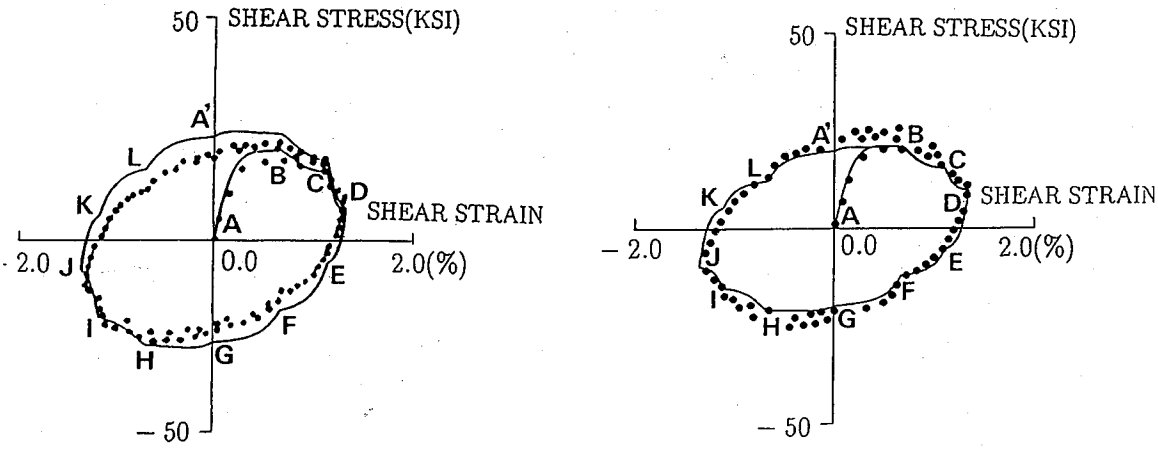

(a) (•) experiment; (–) prediction by Chang[17] (b) (•) experiment; (–) prediction by present model

Fig. 16 Shear stress τ-shear strain γ curves(loading type II)

the model could be used for the local buckling analysis of thin steel plates under cyclic loading, with the consideration of geometric nonlinearity.

REFERENCES

1) Mróz, Z. : On the Description of anisotropic work hardening, *J. Mech. Phys. Solids*, Vol.15, pp.163-175, 1967.

2) Iwan, W.D. : On a class of model for the yielding behavior of continuous and composite system, *Trans., ASME, J. Appl. Mech.*, pp.612-617, Sept. 1967.

3) Petersson, H. and Popov, E.P. : Constitutive relation for generalized loadings, *Proc. of ASCE*, Vol.104, No.EM4, pp.611-627, 1977.

4) Minagawa, M., Nishiwaki, T. and Masuda, N. : Modelling cyclic plasticity of structural steels, *Proc. of JSCE, Structural Eng./Earthquake Eng.*, Vol. 4, No. 2, pp. 361s-370s, 1987.

5) Dafalias, Y.F. and Popov, E.P. : A model of nonlinear hardening materials for complex loading, *Acta, Mech.*, Vol.21, pp.173-192, 1975.

6) Kreig, R.D. : A practical two surface plasticity theory, *ASME Journal of Applied Mechanics*, Vol.42, pp.641-646, 1975.

7) Tseng, N.T. and Lee, G.C. : Simple plasticity model of two-surface type, *Journal of Engineering Mechanics, Proc. ASCE*, Vol.109, NO.3, pp.795-810, June, 1983.

8) Cofie, N.G. and Krawinkler, H. : Uniaxial cyclic stress-strain behavior of structural steel, *Journal of Engineering Mechanics, Proc. ASCE*, Vol.111, No.9, pp.1105-1120, Sept., 1985.

9) Hashiguchi, K. : A mathematical refinement of the two surface model of plasticity, *Proc. of JSCE*, I-4, No.362, pp.259-265, Oct., 1985.

10) McDowell, D. L. : An experimental study of the structure of constitutive equations for nonproportional cyclic plasticity, *ASME, J. Engineering Materials Tech.*, Vol.107, pp.307-315, 1985.

11) Tanaka, Y., Mizuno, E., Shen, C. and Usami, T. : Development of a cyclic two-surface model for steel with yield plateau, *Journal of Structural Engineering*, Vol.37A, pp.1-14, March, 1991(in Japanese).

12) Shen C., Tanaka, Y., Mizuno, E. and Usami, T. : A two-surface model for steels with yield plateau, *Proc. of JSCE, Structural Eng./Earthquake Eng.*, Vol.8, No.4, pp.179s-188s, Jan., 1992.

13) Shen, C., Y., Mizuno, E. and Usami, T. : Further study on two-surface model for structural steels under cyclic loading, *Proc. of JSCE, Structural Eng./Earthquake Eng.*, Vol.9, No.4, pp.257s-260s, Jan., 1993.

14) Chaboche, J.L. : Time-independent constitutive theories for cyclic plasticity, *Int. J. Plasticity*, Vol. 2, pp. 149-188, 1986.

15) Ohno, N. : A constitutive model of cyclic plasticity with a nonhardening strain ragion, *J. of Applied Mechanics, ASME*, Vol.49, pp.721-727, Dec., 1982.

16) O. C. Zienkiewicz : The finite element method, 3rd edition, McGraw-Hill, 1977.

17) Chang, K. C. : Behavior of structural steel under cyclic and nonproportional loading, A dissertation submitted to the Faculty of the Graduate School of State University of New York at Buffalo in partial fulfillment of the requirements for the degree of doctor of philosophy, 1985.

18) Chang, K. C. and Lee, G. C. : Constitutive relations of structural steel under noproportional loading, *J. of Engineering Mechanics, Proc. of ASCE*, Vol.112, No.8, pp.806-820, 1986.

19) Ohno, N., Recent topics in constitutive modeling of cyclic plasticity and visoplasticity, *ASME, Appl. Mech. Rev.*, Vol. 43, 1990.

(Received July 29, 1992)

繰り返し荷重下における構造用鋼材の一般的な二曲面モデル

沈　赤・水野英二・宇佐美勉

本論文では，複合応力状態下の構造用鋼材の繰り返し弾塑性挙動を表現するため，従来の著者らの二曲面モデルをより一般化した二曲面モデルへと拡張した．まず，一軸繰り返し実験から確立した二曲面モデルの概念を一般応力状態のものへと拡張した．さらに，この一般化されたモデルを，有限要素法を用いることにより，二種類の切り欠きを有するＳＳ４００鋼棒の引張・圧縮繰り返し挙動の予測に応用した．また，Non-proportionalな二次元応力径路に対しても，本モデルの有効性について検討した．